*CORRESPONDENCE
Bruce J. Shenker
✉ shenker@upenn.edu

Cellugyrin (synaptogyrin-2) dependent pathways are used by bacterial cytolethal distending toxin and SARS-CoV-2 virus to gain cell entry

Kathleen Boesze-Battaglia[1], Gary H. Cohen[1], Paul F. Bates[2], Lisa M. Walker[1], Ali Zekavat[1] and Bruce J. Shenker[1*]

[1]Department of Basic and Translational Sciences, School of Dental Medicine, University of Pennsylvania, Philadelphia, PA, United States, [2]Department of Microbiology, Perelman School of Medicine, University of Pennsylvania, Philadelphia, PA, United States

Aggregatibacter actinomycetemcomitans cytolethal distending toxin (Cdt) is capable of intoxicating lymphocytes macrophages, mast cells and epithelial cells. Following Cdt binding to cholesterol, in the region of membrane lipid rafts, the CdtB and CdtC subunits are internalized and traffic to intracellular compartments. These events are dependent upon, cellugyrin, a critical component of synaptic like microvesicles (SLMV^{Cg+}). Target cells, such as Jurkat cells, rendered unable to express cellugyrin are resistant to Cdt-induced toxicity. Similar to Cdt, SARS-CoV-2 entry into host cells is initiated by binding to cell surface receptors, ACE-2, also associated with cholesterol-rich lipid rafts; this association leads to fusion and/or endocytosis of viral and host cell membranes and intracellular trafficking. The similarity in internalization pathways for both Cdt and SARS-CoV-2 led us to consider the possibility that cellugyrin was a critical component in both processes. Cellugyrin deficient Calu-3 cells (Calu-3^{Cg-}) were prepared using Lentiviral particles containing shRNA; these cells were resistant to infection by VSV/SARS-CoV-2-spike pseudotype virus and partially resistant to VSV/VSV-G pseudotype virus. Synthetic peptides representing various regions of the cellugyrin protein were prepared and assessed for their ability to bind to Cdt subunits using surface plasmon resonance. Cdt was capable of binding to a region designated the middle outer loop (MOL) which corresponds to a region extending into the cytoplasmic surface of the SLMV^{Cg+}. SARS-CoV-2 spike proteins were assessed for their ability to bind to cellugyrin peptides; SARS-CoV-2 full length spike protein preferentially binds to a region within the SLMV^{Cg+} lumen, designated intraluminal loop 1A. SARS-CoV-2-spike protein domain S1, which contains the receptor binding domains, binds to cellugyrin N-terminus which extends out from the cytoplasmic surface of SLMV. Binding specificity was further analyzed using cellugyrin scrambled peptide mutants. We propose that SLMV^{Cg+} represent a component of a common pathway that facilitates pathogen and/or pathogen-derived toxins to gain host cell entry.

Introduction

Bacterial protein exotoxins and viruses share the ability to hijack host cell pathways for the purposes of gaining cell entry and trafficking to intracellular target sites to achieve toxicity and, in the case of virus, for efficient replication (Harper et al., 2013). Our recent studies suggest that a unique sorting vesicle, cellugyrin (Cg)-positive synaptic-like microvesicles (SLMVs^{Cg+}) mediate entry and subsequent toxicity of bacteria-derived cytolethal distending toxins (Cdts) (Boesze-Battaglia et al., 2016; Boesze-Battaglia et al., 2017; Boesze-Battaglia et al., 2020). Cellugyrin, synaptogyrin-2, is a member of the synaptogyrin tetraspanin protein family (Janz and Sudhof, 1998). Synaptogyrin 1 and 3 are neuronal and are the most abundant proteins in synaptic vesicles; they are critical to vesicle biogenesis, exocytosis and endocytotic recycling as well as neurotransmission (Kedra et al., 1998). Cellugyrin, critical for the biogenesis of SLMVs^{Cg+}, is broadly expressed in all tissue (Human Protein Atlas; https://www.proteinatlas.org/ENSG00000108639-SYNGR2/cell), and is considered to be a critical component of SLMVs^{Cg+} (Janz and Sudhof, 1998; Kupriyanova and Kandror, 2000; Belfort and Kandror, 2003; Kioumourtzoglou et al., 2015). SLMVs^{Cg+} are proposed to be early sorting vesicles and contain proteins essential to endocytic processing and are likely a component of the trans golgi network (TGN) (Janz and Sudhof, 1998). Cytoplasmic SLMVs^{Cg+} are positive for Glut4 (Kupriyanova and Kandror, 2000) and phosphatidylinositol 4-kinase type IIα (Xu et al., 2006). Chapel et al. (2013) have also proposed that cellugyrin may function as a lysosomal transporter protein.

Recently, we determined that cellugyrin plays a requisite role in the internalization and endosomal trafficking of Cdts (Boesze-Battaglia et al., 2016; Boesze-Battaglia et al., 2017; Boesze-Battaglia et al., 2020). To date, we have demonstrated that cellugyrin expression in human lymphocytes, macrophages and, more recently, oral keratinocytes is required for toxin entry and subsequent intoxication of these cells (Boesze-Battaglia et al., 2016; Boesze-Battaglia et al., 2017; Boesze-Battaglia et al., 2020; Shenker et al., 2024). Cdts are produced by more than 30 γ- and ε-Proteobacteria; indeed, we have shown that cellugyrin is required for at least three Cdts produced by *Aggregatibacter actinomycetemcomitans* (*Aa*Cdt), *Haemophilus ducreyi* (*Hd*Cdt) and *Campylobacter jejuni* (*Cj*Cdt) (Boesze-Battaglia et al., 2017; Boesze-Battaglia et al., 2020; Huang et al., 2021). Cdts are heterotrimeric holotoxins that function as AB$_2$ toxins. In this toxin model, the CdtA and CdtC subunits serve as the binding complex (B) and CdtB as the active subunit (A) [reviewed in (Boesze-Battaglia et al., 2016; Scuron et al., 2016)]. Importantly, both CdtB and CdtC are internalized in host target cells such as lymphocytes, macrophages and epithelial cells. The CdtC subunit binds to membrane cholesterol in the context of cholesterol enriched membrane microdomains, or lipid rafts (Boesze-Battaglia et al., 2006; Boesze-Battaglia et al., 2009; Eshraghi et al., 2010; Lin et al., 2011; Zhou et al., 2012; Lai et al., 2013; Boesze-Battaglia et al., 2015; Lai et al., 2015). Within 60 min of exposure to Cdt, cellugyrin translocates from cytoplasm to the plasma membrane in proximity to lipid rafts and associates with CdtB

and CdtC. Immunoprecipitation studies demonstrate that cellugyrin, CdtB and CdtC are associated within a molecular complex found both in purified lipid rafts and in the cytoplasm (Boesze-Battaglia et al., 2017; Boesze-Battaglia et al., 2020).

Similar to bacterial exotoxins, viruses must enter host cells to hijack and alter cell function so that the virus can propagate as viral entry into host cells constitutes the initial steps of the infectious life cycle. For enveloped viruses, this involves binding to host cell receptor(s) followed by fusion and/or endocytosis of viral and host cell membranes and intracellular trafficking, respectively (Gillespie et al., 2013; Nelson et al., 2013; Nonnenmacher et al., 2015; Hartenian et al., 2020). These essential functions are dependent upon viral envelope glycoproteins which are utilized by a number of viruses such as Herpes, SARS-CoV and Ebola to achieve entry and infection of host cells (Eisenberg et al., 2012; Ou et al., 2020). The similarities between pathways utilized to intoxicate cells by both bacterial exotoxins and viruses led us to advance the hypothesis that these pathogens utilize a similar mechanism to achieve cell entry. In this context, we proposed that cellugyrin (specifically SLMV^{Cg+}) acts as a facilitator for the penetration and internalization of either virus or toxin into target host cells. Indeed, we now demonstrate that cells depleted of cellugyrin expression are not only resistant to Cdt intoxication but also viral infection. Moreover, Cdt, as well as two viral proteins, SARS-CoV-2 spike protein and VSV-G protein are capable of binding to cellugyrin-derived peptides. Collectively, these observations support cellugyrin, or more specifically, SLMV^{Cg+} as a critical host cell pathway utilized by some pathogens such as Cdt producing bacteria and virus such as SARS-CoV-2 to gain cell entry.

Materials and methods

Jurkat cells and assessment of Cdt toxicity

The human leukemic T cell line Jurkat was maintained in RPMI 1640 supplemented with 10% FCS, 2 mM glutamine, 10 mM HEPES, 100 U/ml penicillin and 100 g/ml streptomycin as previously described (Shenker et al., 2005). CRISPR/cas9 technology was employed to generate cellugyrin knockout Jurkat cells (Jurkat^{Cg-}) using commercially available reagents (Santa Cruz Biotechnology; Santa Cruz, CA) (Boesze-Battaglia et al., 2017). To measure Cdt-induced cell cycle arrest, Jurkat^{WT} (Jurkat^{Cg+}) and Jurkat^{Cg-} cells were incubated in the presence of medium or Cdt for 16 hr as previously described (Shenker et al., 2000). Briefly, cells were washed and treated with cold 80% ethanol. After washing, cells were stained with 10 μg/ml propidium iodide containing 1 mg/ml RNase (Sigma Chemical Co; St. Louis, MO) for 30 min. Samples were analyzed on a Becton-Dickinson LSR II flow cytometer (BD Biosciences; San Jose, CA). Propidium iodide fluorescence was excited by an argon laser operating at 488nm and fluorescence measured with a 630/22nm bandpass filter using linear amplification. A minimum of 15,000 events were collected on each sample; cell cycle analysis was performed using Modfit (Verity Software House; Topsham, ME).

Calu-3 cells, Lentiviral transfection and pseudotype virus infection

Calu-3 cells were obtained from ATCC and maintained in MEM Alpha containing 10% FBS and 1% pennicillin/ streptomycin (Gibco). Stable cell lines expressing shRNA against cellugyrin (Calu-3[Cg-]) were prepared with commercially available Lentiviral particles (Santa Cruz Biotech; Dallas, TX); cells were transduced with Lentiviral particles as previously described (Abdul-Sater et al., 2010). Briefly, cells (2.5×10^4) were plated and allowed to attach overnight; polybrene (10 μg/mL; Santa Cruz) was added to the cells followed by Lentiviral particles (MOI of 2 - 4; Santa Cruz). After 18 hr, media was replaced with fresh media and cells were allowed to grow for 48 hrs. Calu-3[Cg-] cells were selected by the addition of puromycin (1 μg/mL; Santa Cruz); surviving cells were cloned by limiting dilution and screened by Western blot for cellugyrin content. Cells were maintained with the addition of puromycin (1 μg/mL) in the culture media.

Pseudotyped VSV-ΔGFP/SARS-CoV2-S (Creative-Diagnostics; Shirley, NY USA) encodes the RNA of a replicon-restricted recombinant Vesicular stomatitis virus (rVSV) in which the glycoprotein (G) gene has been replaced with SARS-CoV2 spike gene. The pseudotyped VSV particles encode GPF together with the VSV nucleocapsid, phosphoprotein and large polymerase subunit in their pVSV-ΔG vector. The VSV- RFP/VSV-G pseudotyped virus (kindly provided by Paul F. Bates) expresses RFP and the VSV-G protein (Anderson et al., 2020). For pseudotype virus challenge, cells (10^5) were plated and incubated for 5 days in 24 well plates; Calu-3[Cg-] cells did not receive puromycin for this period. Cells were then challenged with either VSV-ΔRFP/VSV-G or VSV-ΔGFP/ SARS-CoV2-S as indicated in serum free media. After 24 hr, cells were harvested and analyzed using a Becton Dickinson LSR II Flow cytometer. RFP and GFP fluorescence were excited with a 488 laser; fluorescence was monitored using 575/26 and 530/30 filters, respectively.

Surface plasmon resonance

Surface plasmon resonance (SPR) analyses were conducted on a Biacore 3000 (Biacore) at 25°C. The running buffer was PBS containing 0.01 M HEPES (pH 7.4), 3 mM EDTA, and 0.005% surfactant P20 (Biacore). Approximately 2000 response units (RU) of Neutravidin (Thermo Fisher) was coupled to flow cell 2 (Fc2) of a CM5 sensor chip via primary amine coupling according to the manufacturer's specifications. Fc1 was activated and blocked without the addition of protein. Cellugyrin peptides were constructed with N-terminal biotin (Genscript) and diluted to 500 μg/mL in running buffer and run over both flow cells for 4 min at 5 μL/min and the baseline allowed to stabilize. Once stabilized, Cdt holotoxin, individual Cdt subunits, full length SARS-CoV-2 spike protein [(SARS-CoV-2-S[FL]); ACROBiosystems, Newark,DE] and SARS-CoV-2 S1 spike domain [(SARS-CoV-2-S[1]; Genscript] were diluted to concentrations indicated and binding of each sample was monitored for 5 min, with the wash delay set for an additional 5 min to allow for a smooth dissociation curve. The chip surface was regenerated by injecting brief pulses of 0.2 M sodium carbonate (pH 10) until the response signal returned to baseline. The next cycle was started with the injection of a fresh peptide. SPR data were analyzed with BIAevaluation, version 4.1, which employs global fitting.

Statistical analysis

Mean ± standard error of the mean was calculated for replicate experiments. Significance was determined using a Student's t-test with SigmaPlot Software (Systat; San Jose, CA); a P-value of less than 0.05 was considered to be statistically significant.

Results

Cdt and SARS-CoV-2 entry and toxicity is dependent upon cellugyrin

Our recent studies demonstrated that entry of Cdt subunits into human lymphocytes, macrophages and epithelial cells is dependent upon the host cell protein, cellugyrin (Boesze-Battaglia et al., 2017; Boesze-Battaglia et al., 2020). Specifically, we have shown that within 60 min of exposure to Cdt, SLMV[Cg+] translocate to the plasma membrane in proximity to lipid rafts and associates with Cdt subunits CdtB and CdtC. Immunoprecipitation studies also demonstrate that cellugyrin, CdtB and CdtC are associated within a molecular complex found both in purified lipid rafts and in the cytoplasm. Importantly, we have established cell lines with impaired cellugyrin expression for lymphocytes, macrophages and epithelial cells. In all instances, the cellugyrin deficient cells were protected from Cdt toxicity as the active subunit, CdtB was unable to gain intracellular access. An example of this protection is shown in Supplementary Figure 1 which assesses susceptibility of wildtype Jurkat cells (Jurkat[Cg+]), a human lymphoid cell line and cellugyrin deficient Jurkat cells (Jurkat[Cg-]) to toxin-induced cell cycle arrest. Normally, treatment of Jurkat[Cg+] cells with Cdt results in cell cycle arrest represented by an increase in the percentage of cells in the G2/M phases of the cell cycle; this increase is demonstrated in Supplementary Figures 1A, B as the percentage of G2/M cells increased from 11% in cells incubated with medium alone to 50% in the presence of toxin. In contrast, Jurkat[Cg-] cells were resistant to these affects (Supplementary Figures 1C, D) as the percentage of G2/M cells was essentially the same in control (13.7%) and toxin (12.6%) treated cells. Our collective studies to date suggest that cellugyrin is a critical component of a host cell pathway hijacked by Cdt to achieve entry and intoxicate cells.

We now propose that the cellugyrin dependent pathway may also be utilized by viruses to gain cell entry. Here, to demonstrate this relationship we employed the representative pseudotype virus approach for Covid 19. Pseudotype virus was constructed in VSV (lacking VSV-G entry protein) that now contains the SARS-CoV-2 spike protein (VSV-ΔGFP/SARS-CoV-2-S). For comparative purposes we also employed a pseudotype virus which contained the wildtype VSV-G protein (VSV-ΔRFP/VSV-G). The pseudotype

viruses contained either the GFP or RFP gene to facilitate detection. Calu-3 cells, a human epithelial lung cancer cell line, were used as target cells. To determine if viral entry is dependent upon cellugyrin, we generated a Calu-3 cellugyrin deficient cell line (Calu-3^{Cg-}; Figure 1A). Calu-3^{WT} cells were challenged with varying amounts of VSV-ΔGFP/SARS-CoV-2-S pseudotype virus (Figure 1B); 24 hr later cell infection was determined by monitoring GFP fluorescence. Calu-3^{WT} infection was dose-dependent and ranged from 12.0 ± 1.8% infected cells in the presence of 25,000 FFU/ml to 18.8 ± 1.2% in the presence of 100,000 FFU/ml virus. In contrast, Calu-3^{Cg-} cells were totally resistant to infection by VSV-ΔGFP/SARS-CoV-2-S pseudotype virus at all doses; the percentage of infected cells never exceeded the value observed in control (untreated) cells, 0.95 ± 0.1%. Calu-3 cells were also challenged with VSV-ΔRFP/VSV-G (0-100,000 FFU/ml) (Figure 1C); 24 hr later cells were analyzed for infection by monitoring RFP fluorescence. Calu-3^{WT} cells were infected in a dose-dependent manner; 8.9 ± 0.8% cells were infected when exposed to 12,500 FFU; the percentage increased with each dose of virus to a maximum of 25.4 ± 2.9% in the presence of 100,000 FFU/ml, the highest viral concentration employed. In contrast, Calu-3^{Cg-} cells exhibited significantly reduced infection when challenged with the same doses of pseudotype virus (12,500 to 100,000): 3.1 ± 0.7%, 5.0 ± 1.0%, 7.6 ± 1.4% and 11.9 ± 2.9%.

Cdt binds to cellugyrin peptides

Previously, we demonstrated that Cdt subunits co-localize with cellugyrin in the vicinity of cholesterol-rich microdomains in both human lymphocytes and macrophages and, as noted above, form molecular complexes detected by immunoprecipitation (Boesze-Battaglia et al., 2017; Boesze-Battaglia et al., 2020). Prior to our current studies, we had not demonstrated direct binding between the Cdt subunits and cellugyrin. We now assessed the ability of Cdt holotoxin and individual subunits to bind directly to synthetic cellugyrin peptides; these analyses not only allow us to identify regions of cellugyrin association but also to predict the binding site location within the context of SLMV^{Cg+}. For this purpose, peptides were designed based upon cellugyrin sequence and topography within SLMV^{Cg+}; a topology model for cellugyrin within SLMV^{Cg+} is presented in Figure 2 (Stenius et al., 1995; Low et al., 2012). In this rendition, the N-terminus and C-terminus extend into the cytoplasm; the middle outer loop (MOL) links transmembrane (TM) regions TM2 with TM3 and is exposed to the cytoplasmic surface of SLMV^{Cg+} as well. Additionally, there are two loops within the lumen of SLMV^{Cg+} designated inner loop (IL) 1 (IL1) which links TM1 and TM2 and IL2 which links TM3 and TM4.

Based on these predictions, seven peptides, corresponding to each of the inner and outer cellugyrin loop domains as well as both the N– and C-terminus, were designed and synthesized as described in Materials and Methods (Table 1; Figure 2). Due to length of the IL1 loop and C-terminus, two peptides covering this region were designed and designated IL1, IL1A, C-Term 1 and C-Term 2. SPR (Biacore) was employed to assess Cdt subunit and holotoxin binding to the immobilized cellugyrin peptides. Analysis of the

binding of Cdt holotoxin, containing all three subunits indicated maximum binding to the MOL peptide (Figure 2A). While the Cdt holotoxin exhibited binding to all peptides, preferential binding (maximum RU 380) was observed with the MOL peptide. Similarly, the Cdt binding subunit, CdtC, also exhibited the highest RU (340) with the MOL peptide (Figure 2B); moderate interactions were observed with IL1, IL1A and IL2. No interactions were observed with the N-Term or with either of the two C-Term peptides. Also, we did not detect interactions with any of the cellugyrin peptides when the CdtB subunit and CdtA subunit were assessed individually (data not shown).

We next tested criteria for peptide binding and specificity with the MOL region (Figure 3). Specifically, we employed MOL mutant peptides in which isoelectric point was altered and aromatic resides were replaced with alanine, individually and in combination, as illustrated in Figure 3. Cdt holotoxin bound to cellugyrin MOL MUT2; in this mutant basic residues were replaced with alanine leading to a marked reduction of the isoelectric point from 6.8 to 2.9. Binding however, was only 50% of the maximum RU when compared to the native peptide (Figure 3A). Binding of the holotoxin was abolished with all other peptide combinations (MOL MUT3-MUT6). When CdtC binding was assessed using the same panel of cellugyrin MOL mutants, binding was abolished when aspartic acid (D) residues were replaced by alanine regardless of whether phenylalanine (F) was also replaced (MOL MUT2 and MOL MUT3; Figure 3B). Binding to MOL MUT5 in which the phenylalanine was retained, while lower than native peptide was measurable, inferring the essentiality of aspartic acid. Collectively, these series of mutant MOL studies suggest that the interaction between Cdt holotoxin as well as the Cdt C subunit may rely on charged amino acid residues. Going forward we will assess the contribution of the individual charged residues, both acidic and basic, to optimal Cdt-cellugyrin association.

SARS-CoV-2 binds to cellugyrin peptides

Next, we used a similar approach to assess the ability of viral proteins to bind to cellugyrin peptides; these included full length SARS-CoV-2 spike protein (SARS-CoV-2-S$_{FL}$), SARS-CoV-2 spike domain 1 containing the RBD (SARS-CoV-2-S$_1$) and VSV-G. SARS-CoV-2-S$_{FL}$ exhibited binding to IL1A with a maximum RU of 220 (Figure 4A); low binding was observed with the other peptides exhibiting a maximum RU range of 55 to 95. It should be noted that IL1 and IL1A collectively represent the inner loop 1 region with minimal overlap. In contrast, SARS-CoV2-S$_1$ preferentially bound to the N-Term peptide with a maximum RU of 530 (Figure 4B); this protein also exhibited binding to the other peptides with lower RUs ranging from 50 to 380. VSV-G exhibited maximal binding to the MOL peptide with a peak RU of 140 (Supplementary Figure 2A).

Similar to our approach to understanding the specificity of Cdt binding to cellugyrin peptides, we also generated mutant peptides corresponding to regions of interaction between cellugyrin and SARS-CoV-2-S$_{FL}$ (IL1A) and SARS-CoV-2-S$_1$ (N-Term) (Figure 5). IL1A mutant peptides represent changes in charged and cysteine
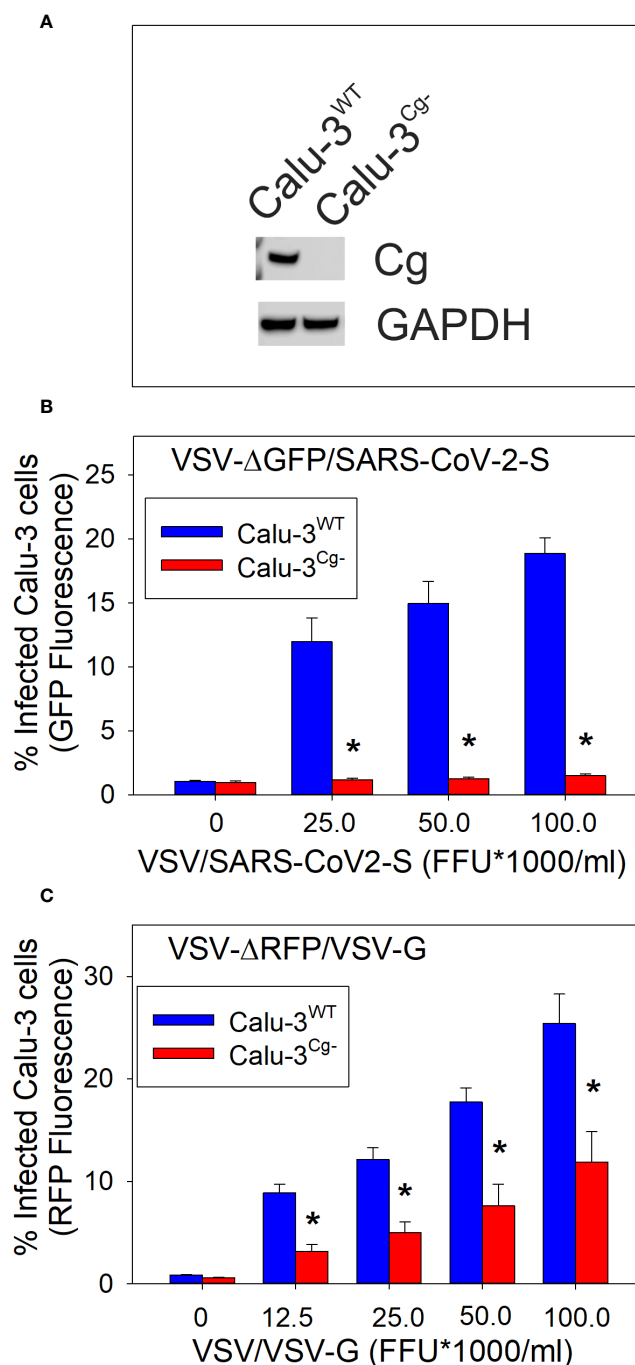
FIGURE 1

Calu-3 cell susceptibility to SARS-CoV-2 infection is cellugyrin dependent. Calu-3 cells deficient in cellugyrin expression (Calu-3^Cg-) were generated using Lentiviral particles as described in Materials and Methods. As shown in panel **(A)** cellugyrin expression was not detectable in Calu-3^Cg- cells by Western blot analysis. Correspondingly, the susceptibility of Calu-3^WT (Calu-3^Cg+; blue bars) and Calu-3^Cg- (red bars) cells to infection by VSV-ΔGFP/ SARS-CoV-2-S pseudotyped virus (panel **B**) or to VSV-RFP/VSV-G pseudotyped virus (panel **C**) were assessed. Cells were challenged with varying FFU for 24 hrs and then analyzed for GFP or RFP fluorescence by flow cytometry. The concentration of FFU is plotted versus the percentage of cells exhibiting increased GFP fluorescence; results are the mean ± SEM of three experiments. *indicates statistical significance (p<0.05).

residues (Figure 5A). In IL1A MUT1, cysteine was replaced with alanine, in IL1A MUT2 and IL1A MUT3, hydrophobicity and charge were decreased; in IL1A MUT3 we also replaced cysteine with alanine. SARS-CoV-2-S$_{FL}$ binding to IL1A MUT1 and IL1A MUT2 was reduced by more than 50% relative to the wildtype peptide (Figure 5A). In IL1A MUT3, both the cysteine residues and

tyrosine residues were replaced with alanine leading to a 70% decrease in SARS-CoV-2-S$_{FL}$ binding. Collectively, these studies suggest that SARS-CoV-2-S$_{FL}$ relies on a combination of cysteine and aromatic residues for maximal binding The potential importance of a disulfide bridge will be considered in future studies. The N-terminal mutant peptides were assessed and
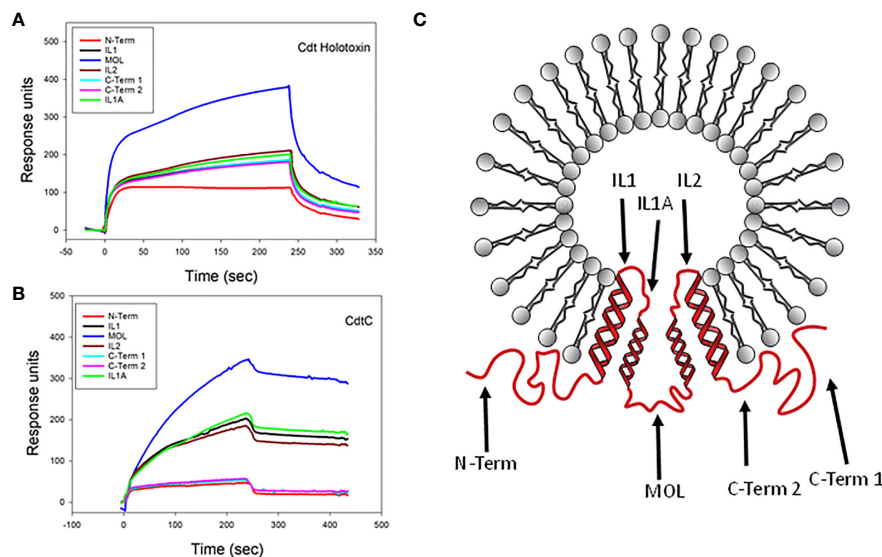
FIGURE 2
SPR analysis of Cdt binding to cellugyrin peptides. The interaction of Cdt holotoxin **(A)** and CdtC **(B)** with the seven cellugyrin peptides were analyzed by SPR. Representative sensorgrams for the interaction of Cdt holotoxin (1.0 µM) and CdtC (4.0 µM) with cellugyrin peptides are shown and plotted as response units versus time. Sensorgrams are representative of at least three repetitive experiments. **(C)** shows a topographical model of cellugyrin within SLMV[Cg+]. Cellugyrin is shown in red along with the 7 peptides that were designed (black arrows): N-terminus (N-Term), C-terminus (C-Term) 1 and C-Term 2 and middle loop (MOL) face the cytoplasmic surface of the vesicles. The intraluminal loops (IL) are designated IL, IL1A and IL2. Additionally, the four transmembrane regions (TM1-4) are shown. Adapted from Low et al. (2012).

modified as follows (Figure 5B): N-Term MUT1 hydrophobicity was reduced and N-Term MUT2 isoelectric point was lowered (Figure 3). SARS-CoV-2-S₁ exhibited a 25% reduction in binding with N-Term MUT1 while loss of both hydrophobicity and basic charge (lysine) abolished binding in N-Term MUT2 (Figure 5B).

VSV-G binding to MOL mutants was assessed using the same mutant peptides as employed above for Cdt holotoxin and CdtC (Figure 3). Similar to Cdt holotoxin and CdtC, VSV-G binding was abolished with MOL MUT5 and MOL MUT6 (Supplementary Figure 2B), The other MOL mutants exhibited 30-50% reduced binding based on maximal RU.

Additional SPR analyses were conducted to determine binding affinities for each of the pathogen proteins with the cellugyrin peptide to which they exhibited preferential reactivity as described above. Figure 6 shows representative series of overlay sensorgram responses for multiple concentrations of Cdt holotoxin

(Figure 6A) and CdtC subunit (Figure 6B) binding to MOL. Both actual data (solid lines) and modeled data (dashed lines) are plotted. K_D values were calculated for Cdt holotoxin and CdtC binding to the MOL as $1.73 \pm 0.46 \times 10^{-3}$ M and $3.7 \pm 1.5 \times 10^{-4}$ M, respectively. Similarly, sensorgram overlays for varying concentrations of each of the viral proteins are shown for SARS-CoV-2-S_{FL} binding to IL1A (Figure 6C) and SARS-CoV-2-S_1 binding to N-term (Figure 6D); the calculated K_D values are $4.53 \pm 0.48 \times 10^{-3}$ M, $5.63 \pm 1.54 \times 10^{-4}$ M, respectively.

Discussion

Cdt is able to intoxicate multiple host cell types by virtue of its exploitation of a ubiquitous cell receptor, cholesterol, and its molecular mode of action which disrupts phosphatidylinositol-3 kinase (PI-3K) signaling by enzymatically depleting cells of PIP3 (Boesze-Battaglia et al., 2006; Shenker et al., 2007; Boesze-Battaglia et al., 2009; Shenker et al., 2010; Shenker et al., 2014; Boesze-Battaglia et al., 2015). Moreover, following CdtC binding to cholesterol, internalization and intracellular trafficking of CdtB involves utilization of the host protein, cellugyrin (Boesze-Battaglia et al., 2017; Boesze-Battaglia et al., 2020). In the absence of cellugyrin, CdtB does not enter cells and is unable to induce toxicity. Moreover, we have previously demonstrated that Cdts derived from *Haemophilus ducreyi* and *Campylobacter jejuni* are also dependent upon cellugyrin for entry and toxicity (Huang et al., 2021). In this study we demonstrate for the first time that both Cdt holotoxin and the toxin's CdtC cholesterol binding subunit directly interact with cellugyrin. Specifically, these toxin entities bind to the

TABLE 1 Cellugyrin peptides.

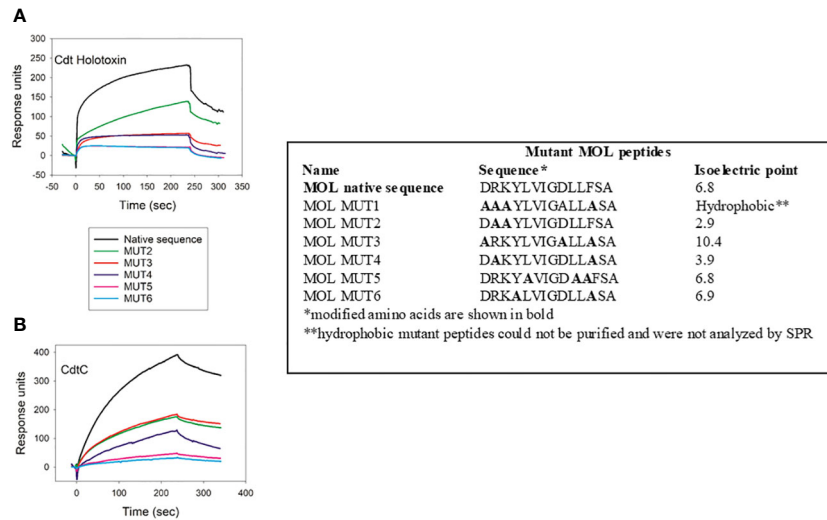| Name	Sequence
N-Term	[2]ESGAYGAAKAGGSF[15]
Inner loop 1 (IL1)	[45]GEGYSNAHESKQMYC[59]
Inner loop 1A (ILA)	[57]MYCVFNRNEDACRYG[71]
Middle outer loop (MOL)	[100]DRKYLVIGDLLFSA[113]
Inner loop 2 (IL2)	[125]LTNQWAVTNPKDVLVGAD[143]
C-Term 1	[173]GVDDFIQNYVDPTPDP[188]
C-Term 2	[211]NAETTEGYQPPPVY[224]

FIGURE 3

Charged amino acid residues in cellugyrin MOL are necessary for Cdt binding. The interaction of 1 μM Cdt holotoxin **(A)** and 4.0 μM CdtC **(B)** with MOL mutant peptides was analyzed by SPR. Sequence of mutated peptides and change in pI are shown. Representative sensorgrams for the interaction of Cdt proteins with wildtype and mutant MOL peptides are shown and plotted as response units versus time. Sensorgrams are representative of at least two repetitive experiments.

peptide containing a sequence that corresponds to a region representing the MOL; it is noteworthy that this region resides on the cytoplasmic surface of SLMV[Cg+] (see Figure 2C). Moreover, we have previously shown that SLMV[Cg+] accumulate within the cholesterol rich lipid membrane rafts following exposure to Cdt.

The relative affinity for the MOL peptide was determined to be higher for the CdtC subunit than that observed for the holotoxin (K_D values were $3.71 \pm 1.50 \times 10^{-4}$ M and $1.73 \pm 0.46 \times 10^{-3}$ M, respectively). We did not detect significant binding of the CdtA subunit and the active Cdt subunit, CdtB, to cellugyrin peptides
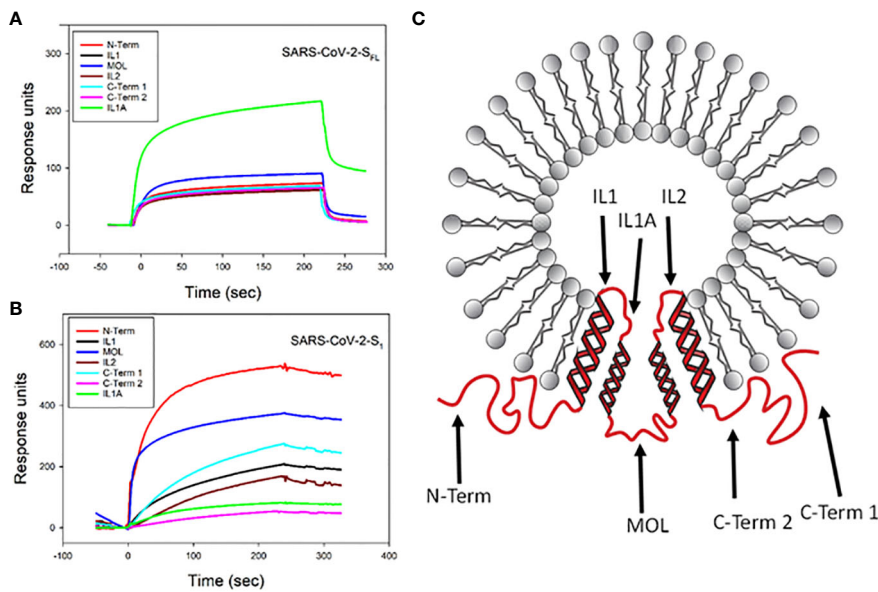

FIGURE 4

SPR analysis of viral protein binding to cellugyrin peptides. The interaction of 2.5 μM SARS-CoV-2-S$_{FL}$ **(A)** and 2.5 μM SARS-CoV-2-S$_1$ **(B)** with cellugyrin peptides were analyzed by SPR. Sensorgrams for the interaction of viral proteins with cellugyrin peptides are shown and plotted as response units versus time. Sensorgrams are representative of at least three repetitive experiments. **(C)** shows a topographical model of cellugyrin within SLMVCg+. Cellugyrin is shown in red along with the 7 peptides that were designed (blue arrows): N-terminus (N-Term), C-terminus (C-Term) 1 and C-Term 2 and middle loop (MOL) face the cytoplasmic surface of the vesicles. The intraluminal loops (IL) 1, IL1A and IL2. Additionally, the four transmembrane regions (TM1-4) are shown. Adapted from Low et al. (2012).
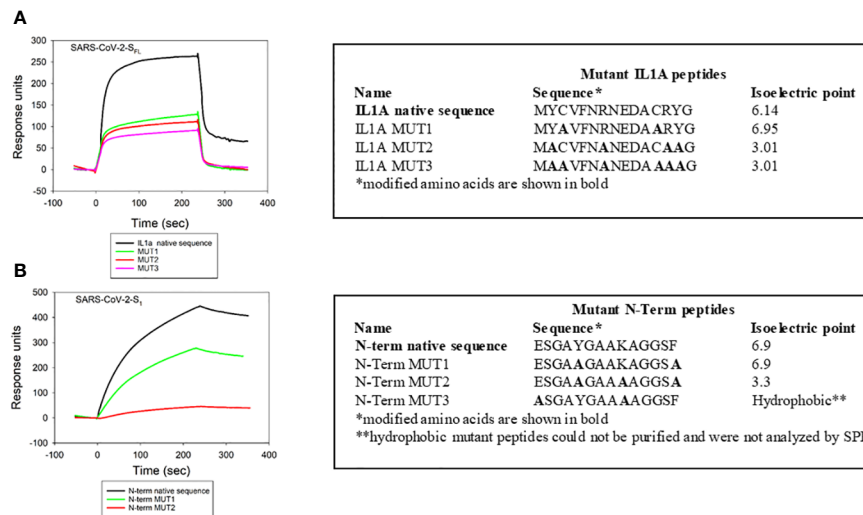
FIGURE 5
Viral protein binding to cellugyrin is dependent on charged amino acid residues. The interaction of 2.5 µM SARS-CoV-2-S_{FL} with IL1A mutants **(A)** and 2.5 µM SARS-CoV-2-S_1 with N-Term mutants **(B)** was analyzed by SPR. Mutation sequences and how they deviate from native protein sequence is shown. Representative sensorgrams of at least two repetitive experiments are shown for the interaction of viral proteins with wildtype and mutant IL1A and N-Term peptides are shown and plotted as response units versus time.

(data not shown). However, it should be noted that CdtB entry is not only dependent upon CdtC, but both subunits enter cells and initially remain part of a multi-protein-cellugyrin positive complex detectable by immunoprecipitation (Boesze-Battaglia et al., 2017). Moreover, it is possible that CdtB binding to cellugyrin may involve

cellugyrin sequences not represented within the pool of peptides employed in the current study. It should also be noted that the inability of the CdtA subunit, also a cell surface binding subunit, to interact with cellugyrin is consistent with the observation that this subunit does not enter host cells (Boesze-Battaglia et al., 2017). In
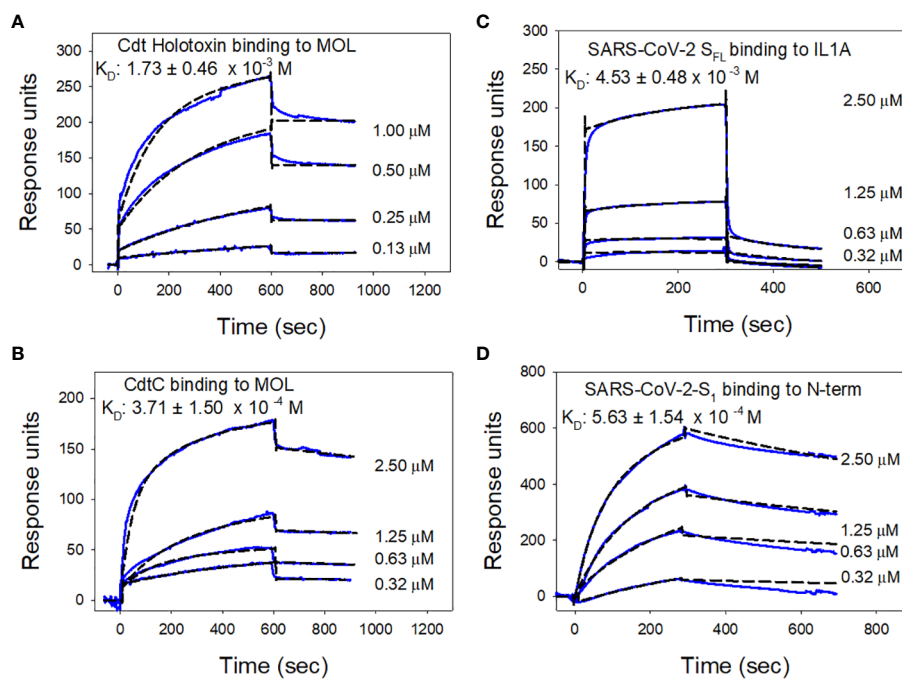

FIGURE 6
Analysis of toxin and viral protein binding affinities to cellugyrin peptides. Representative sensorgrams for the interaction of various concentrations of Cdt holotoxin **(A)** and CdtC **(B)** to MOL is shown. Sensorgrams for the interaction of various concentrations of SARS-CoV-2-S_{FL} with IL1A **(C)** and SARS-CoV-2-S_1 with N-Term **(D)** are shown. Experimental line (solid) is shown along with the model fit (broken line). K_D values were calculated from these data and the mean $\pm$ SEM of three experiments are shown in each panel; sensorgrams are representative of at least three repetitive experiments.

addition to our previous studies demonstrating that CdtB requires cellugyrin for internalization and intoxication of host cells, we now demonstrate and identify regions of direct interaction between toxin and the host cell protein cellugyrin.

Viral entry into host cells follows a similar pattern to that described above for bacterial exotoxins such as Cdts: recognition and binding to host cell receptors, translocation across the plasma membrane and hijacking of intracellular transport mechanisms (Eisenberg et al., 2012; Glebov, 2020; Hartenian et al., 2020; Scudellari, 2021). In this regard, SARS-CoV-2 expresses a spike protein (S) with three receptor-binding heads (S1) that sit on top of a fusion stalk (S2). S1 contains the receptor binding domain (RBD) that specifically recognizes angiotensin-converting enzyme 2 (ACE2) as it's host cell receptor. Following RBD binding to ACE2, viral and host cell membrane fusion takes place; this process involves host cell protease-dependent modification of S2 (which is able to function as a fusogen) following its dissociation from S1 (Ou et al., 2020; Shang et al., 2020; Wan et al., 2020). Following fusion, endosome formation and maturation leads to release of viral RNA and hijacking of the protein synthetic machinery of the cell to synthesize viral proteins that ultimately assemble into more copies of the virus. Another similarity worth noting between SARS-CoV-2 (and SARS-CoV) interaction with host cells and that observed for Cdt is that cell entry involves interactions associated with membrane lipid rafts (Li et al., 2007; Lu et al., 2008; Fecchi et al., 2020) as ACE-2 has been reported to associate within these cholesterol-rich membrane regions. The requirement for the integrity of these regions was further shown by the observation that cholesterol depletion protects cells from viral entry; similar observations have been made for Cdt (Boesze-Battaglia et al., 2009; Eshraghi et al., 2010; Lin et al., 2011; Lai et al., 2013; Boesze-Battaglia et al., 2015; Boesze-Battaglia et al., 2016). These similarities to Cdt entry led us to consider the possibility that SARS-CoV-2 might also interact with, and be dependent upon, cellugyrin.

Clearly, our observations demonstrate that cellugyrin is critical for SARS-CoV-2 infection as we demonstrated that cells with impaired expression of this protein (Calu-3^{Cg-} cells) were resistant to infection by VSV-ΔGFP/SARS-CoV-2-S pseudotype virus. SARS-CoV-2-S$_{FL}$ binds to the cellugyrin peptide containing an amino acid sequence corresponding to IL1A with a similar affinity as the Cdt proteins (K_D 4.53 ± 0.48 x 10^{-3} M). This region is present within the vesicle lumen (Figure 4C); access to this region of the tetraspanin protein is likely consistent with fusion processes that have been proposed for the early stages of viral entry. Indeed, the involvement of fusion with SLMV^{Cg+} is supported by the observation that these vesicles contain the v-SNARE fusion protein (Kupriyanova and Kandror, 2000). SLMV^{Cg+} have been shown to traffic to the plasma membrane under basal conditions; this association and likely subsequent fusion is mediated through a plasma membrane associated t-SNARE (Kioumourtzoglou et al., 2015). Moreover, SLMV^{Cg+} fusion with the plasma membrane has been demonstrated in response to insulin signaling to deliver GLUT4 (Kupriyanova and Kandror, 2000; Kupriyanova et al., 2002). Interestingly, the spike S1 domain preferentially binds to the N-terminus which extends from the SLMV^{Cg+} surface into the cytoplasm (K_D 5.63 ± 1.540 x 10^{-4} M). Collectively, these observations allow for the possibility of two-stage interaction between SARS-CoV-2 spike protein and cellugyrin. For example, initial viral-cellugyrin binding may involve the S1 domain of the spike protein binding to the N-terminus of cellugyrin; this may be followeded by fusion and/or reorganization of the SLMV^{Cg+} allowing for interaction with the IL1A region (Figure 7). Clearly, future studies will focus on advancing our understanding of the involvement of these regions in SARS-CoV-2 infection.

We also assessed the VSV-G protein for its ability to interact with cellugyrin. The VSV-G protein, similar to the SARS-CoV-2 spike protein, is required for binding to host cell receptors and subsequent internalization and cell infection (Oksayan et al., 2012; Regan and Whittaker, 2013). Interestingly, VSV-G, like Cdt holotoxin and CdtC, preferentially binds to the MOL. In contrast to our observations with VSV-ΔGFP/SARS-CoV-2, Calu-3^{Cg-} cells were partially protected from infection with the VSV-ΔRFP/VSV-G pseudotype virus. Failure to totally block VSV-ΔRFP/VSV-G pseudotype viral entry likely reflects VSV's known ability to utilize multiple pathways to gain host cell entry (Oksayan et al., 2012; Regan and Whittaker, 2013).

There is additional evidence in support of cellugyrin, or more specifically SLMV^{Cg+}, serving as a critical host cell protein utilized by viruses for the purposes of intracellular trafficking and infection. For example, Sun et al. (2016) reported on the role of cellugyrin in the infection of mammalian cells by Bunyavirus which is responsible for severe fever with thrombocytopenia syndrome virus (SFTSV). Cellugyrin was shown to interact with nonstructural viral proteins and further, these interactions led to the transport of these proteins into inclusion bodies that were "reconstructed from lipid droplets" during viral infection. The importance of this translocation was demonstrated by silencing cellugyrin expression which resulted in reduced inclusion body formation and viral titers. More recently, Walker et al. (2018) reported on Porcine circovirus 2 (PCV2) which is responsible for a group of diseases known as PCV2 Associated Disease. PCV2 disease exhibits variation in incidence and severity of disease; investigators proposed that this variability is due to missense mutation in the SYNGR2 gene (cellugyrin) resulting in altered viremia. Experimental silencing of SYNGR expression was found to significantly reduce PCV2 titers in infected PK15 cells. It was proposed that cellugyrin mutation(s) affect virus incorporation into vesicular membranes and thereby alter vesicle formation; the altered vesicles fail to transport PCV2 resulting in impaired viral replication.

The observations reported in this study led us to propose that similar to exotoxins such as Cdt, viruses such as SARS-CoV-2 hijack the cellugyrin-dependent pathway to access intracellular compartments within host target cells. Noteworthy, in a recent study on the upper airway host transcriptional response of patients with COVID-19 to other viral lung infections SYNGR2 was found to be upregulated >1.035-fold and 1.35-fold when compared with nonviral respiratory disorders (Mick et al., 2020). In light of our
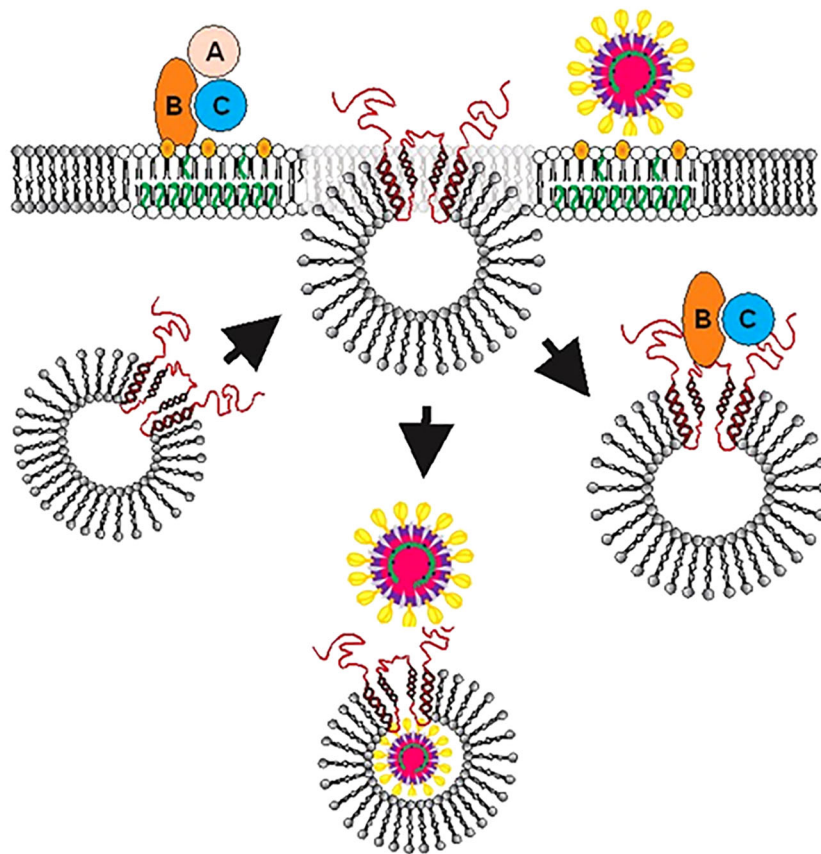
FIGURE 7
Proposed model for the role of SLMV^{Cg+} in facilitating Cdt or viral entry into host cells and intracellular trafficking. After binding of toxin (Top left) or virus (Top right) to lipid raft associated receptors, SLMV^{Cg+} translocate from cytoplasm to plasma membrane allowing cellugyrin (red) to be exposed to the extracellular surface and associate with pathogen binding proteins. For viruses such as SARS-CoV-2 we further propose that a second step (also occurring in close proximity to the plasma membrane) involves fusion events that ultimately lead to viral translocation to the SLMV^{Cg+} lumen. Orange represents cholesterol and green unsaturated fatty acids within the host cell membrane.

current observations with the bacterial exotoxin, Cdt, and SARS-CoV-2, we now propose that SLMV^{Cg+}, and cellugyrin in particular, represent a universal facilitator for an array of pathogens, or their virulence factors, to achieve host cell entry. Moreover, a developing theme in these interactions is the involvement of cholesterol-rich microdomains as a region in which pathogen, host cell receptor and cellugyrin likely come together to initiate the internalization process (es). In conclusion, our study provides evidence that viruses and exotoxins alike, utilize a *common mechanism* to achieve cell entry (Figure 7). We propose that hijacking of this SLMV^{Cg+} pathway is a requisite for both bacterial and viral infection which leads to altered host cell function which, in turn, contributes to disease pathogenesis. Clearly, modulation of cellugyrin expression or interference with pathogen-cellugyrin interaction represent novel, non-anti-microbial, approaches to prevent and/or treat a range of viral and bacterial-induced disorders.

Data availability statement

The raw data supporting the conclusions of this article will be made available by the authors, without undue reservation.

Author contributions

KB-B: Conceptualization, Data curation, Formal analysis, Funding acquisition, Investigation, Methodology, Project administration, Resources, Supervision, Validation, Visualization, Writing – original draft, Writing – review & editing. GC: Conceptualization, Formal analysis, Methodology, Writing – review & editing. PB: Methodology, Resources, Writing – review & editing. LW: Data curation, Formal analysis, Investigation, Methodology, Writing – review & editing. AZ: Data curation, Formal analysis, Investigation, Methodology, Writing – review & editing. BS: Conceptualization, Data curation, Formal analysis, Funding acquisition, Investigation, Methodology, Project administration, Resources, Supervision, Validation, Visualization, Writing – original draft, Writing – review & editing.

Funding

National Institute of Dental and Craniofacial Research at the National Institutes of Health

Acknowledgments

The authors wish to acknowledge the support and expertise of the PDM Flow Cytometry Facility and Confocal Core Facility.

Conflict of interest

The authors declare that the research was conducted in the absence of any commercial or financial relationships that could be construed as a potential conflict of interest.

Publisher's note

All claims expressed in this article are solely those of the authors and do not necessarily represent those of their affiliated organizations, or those of the publisher, the editors and the reviewers. Any product that may be evaluated in this article, or claim that may be made by its manufacturer, is not guaranteed or endorsed by the publisher.

Supplementary material

The Supplementary Material for this article can be found online at: https://www.frontiersin.org/articles/10.3389/fcimb.2024.1334224/full#supplementary-material

References

Abdul-Sater, A. A., Said-Sadier, N., Padilla, E. V., and Ojcius, D. M. (2010). Chlamydial infection of monocytes stimulates IL-1beta secretion through activation of the NLRP3 inflammasome. *Microbes Infect.* 12, 652–661. doi: 10.1016/j.micinf.2010.04.008

Anderson, E. M., Diorio, C., Goodwin, E. C., McNerney, K. O., Weirick, M. E., Gouma, S., et al. (2020). SARS-CoV-2 antibody responses in children with MIS-C and mild and severe COVID-19. *medRxiv.* doi: 10.1101/2020.08.17.20176552

Belfort, G. M., and Kandror, K. V. (2003). Cellugyrin and synaptogyrin facilitate targeting of synaptophysin to a ubiquitous synaptic vesicle-sized compartment in PC12 cells. *J. Biol. Chem.* 278, 47971–47978. doi: 10.1074/jbc.M304174200

Boesze-Battaglia, K., Alexander, D., Dlakic, M., and Shenker, B. J. (2016). A journey of cytolethal distending toxins through cell membranes. *Front. Cell Infect. Microbiol.* 6, 81. doi: 10.3389/fcimb.2016.00081

Boesze-Battaglia, K., Besack, D., McKay, T., Zekavat, A., Otis, L., Jordan-Sciutto, K., et al. (2006). Cholesterol-rich membrane microdomains mediate cell cycle arrest induced by Actinobacillus actinomycetemcomitans cytolethal-distending toxin. *Cell Microbiol.* 8, 823–836. doi: 10.1111/j.1462-5822.2005.00669.x

Boesze-Battaglia, K., Brown, A., Walker, L., Besack, D., Zekavat, A., Wrenn, S., et al. (2009). Cytolethal distending toxin-induced cell cycle arrest of lymphocytes is dependent upon recognition and binding to cholesterol. *J. Biol. Chem.* 284, 10650–10658. doi: 10.1074/jbc.M809094200

Boesze-Battaglia, K., Dhingra, A., Walker, L. M., Zekavat, A., and Shenker, B. J. (2020). Internalization and intoxication of human macrophages by the active subunit of the aggregatibacter actinomycetemcomitans cytolethal distending toxin is dependent upon cellugyrin (Synaptogyrin-2). *Front. Immunol.* 11, 1262. doi: 10.3389/fimmu.2020.01262

Boesze-Battaglia, K., Walker, L. P., Dhingra, A., Kandror, K., Tang, H. Y., and Shenker, B. J. (2017). Internalization of the Active Subunit of the Aggregatibacter actinomycetemcomitans Cytolethal Distending Toxin Is Dependent upon Cellugyrin (Synaptogyrin 2), a Host Cell Non-Neuronal Paralog of the Synaptic Vesicle Protein, Synaptogyrin 1. *Front. Cell Infect. Microbiol.* 7, 469. doi: 10.3389/fcimb.2017.00469

Boesze-Battaglia, K., Walker, L. P., Zekavat, A., Dlakic, M., Scuron, M. D., Nygren, P., et al. (2015). The aggregatibacter actinomycetemcomitans cytolethal distending toxin active subunit cdtB contains a cholesterol recognition sequence required for toxin binding and subunit internalization. *Infect. Immun.* 83, 4042–4055. doi: 10.1128/IAI.00788-15

Chapel, A., Kieffer-Jaquinod, S., Sagne, C., Verdon, Q., Ivaldi, C., Mellal, M., et al. (2013). An extended proteome map of the lysosomal membrane reveals novel potential transporters. *Mol. Cell Proteomics* 12, 1572–1588. doi: 10.1074/mcp.M112.021980

Eisenberg, R. J., Atanasiu, D., Cairns, T. M., Gallagher, J. R., Krummenacher, C., and Cohen, G. H. (2012). Herpes virus fusion and entry: a story with many characters. *Viruses* 4, 800–832. doi: 10.3390/v4050800

Eshraghi, A., Maldonado-Arocho, F. J., Gargi, A., Cardwell, M. M., Prouty, M. G., Blanke, S. R., et al. (2010). Cytolethal distending toxin family members are differentially affected by alterations in host glycans and membrane cholesterol. *J. Biol. Chem.* 285, 18199–18207. doi: 10.1074/jbc.M110.112912

Fecchi, K., Anticoli, S., Peruzzu, D., Iessi, E., Gagliardi, M. C., Matarrese, P., et al. (2020). Coronavirus interplay with lipid rafts and autophagy unveils promising therapeutic targets. *Front. Microbiol.* 11, 1821. doi: 10.3389/fmicb.2020.01821

Gillespie, E. J., Ho, C. L., Balaji, K., Clemens, D. L., Deng, G., Wang, Y. E., et al. (2013). Selective inhibitor of endosomal trafficking pathways exploited by multiple toxins and viruses. *Proc. Natl. Acad. Sci. U.S.A.* 110, E4904–E4912. doi: 10.1073/pnas.1302334110

Glebov, O. O. (2020). Understanding SARS-CoV-2 endocytosis for COVID-19 drug repurposing. *FEBS J.* 287, 3664–3671. doi: 10.1111/febs.15369

Harper, C. B., Popoff, M. R., McCluskey, A., Robinson, P. J., and Meunier, F. A. (2013). Targeting membrane trafficking in infection prophylaxis: dynamin inhibitors. *Trends Cell Biol.* 23, 90–101. doi: 10.1016/j.tcb.2012.10.007

Hartenian, E., Nandakumar, D., Lari, A., Ly, M., Tucker, J. M., and Glaunsinger, B. A. (2020). The molecular virology of coronaviruses. *J. Biol. Chem.* 295, 12910–12934. doi: 10.1074/jbc.REV120.013930

Huang, G., Boesze-Battaglia, K., Walker, L. P., Zekavat, A., Schaefer, Z. P., Blanke, S. R., et al. (2021). The Active Subunit of the Cytolethal Distending Toxin, CdtB, Derived From Both Haemophilus ducreyi and Campylobacter jejuni Exhibits Potent Phosphatidylinositol-3,4,5-Triphosphate Phosphatase Activity. *Front. Cell Infect. Microbiol.* 11, 664221. doi: 10.3389/fcimb.2021.664221

Janz, R., and Sudhof, T. C. (1998). Cellugyrin, a novel ubiquitous form of synaptogyrin that is phosphorylated by pp60c-src. *J. Biol. Chem.* 273, 2851–2857. doi: 10.1074/jbc.273.5.2851

Kedra, D., Pan, H. Q., Seroussi, E., Fransson, I., Guilbaud, C., Collins, J. E., et al. (1998). Characterization of the human synaptogyrin gene family. *Hum. Genet.* 103, 131–141. doi: 10.1007/s004390050795

Kioumourtzoglou, D., Pryor, P. R., Gould, G. W., and Bryant, N. J. (2015). Alternative routes to the cell surface underpin insulin-regulated membrane trafficking of GLUT4. *J. Cell Sci.* 128, 2423–2429. doi: 10.1242/jcs.166561

Kupriyanova, T. A., and Kandror, K. V. (2000). Cellugyrin is a marker for a distinct population of intracellular Glut4-containing vesicles. *J. Biol. Chem.* 275, 36263–36268. doi: 10.1074/jbc.M002797200

Kupriyanova, T. A., Kandror, V., and Kandror, K. V. (2002). Isolation and characterization of the two major intracellular Glut4 storage compartments. *J. Biol. Chem.* 277, 9133–9138. doi: 10.1074/jbc.M106999200

Lai, C. H., Lai, C. K., Lin, Y. J., Hung, C. L., Chu, C. H., Feng, C. L., et al. (2013). Characterization of putative cholesterol recognition/interaction amino acid consensus-like motif of Campylobacter jejuni cytolethal distending toxin C. *PLoS One* 8, e66202. doi: 10.1371/journal.pone.0066202

Lai, C. K., Su, J. C., Lin, Y. H., Chang, C. S., Feng, C. L., Lin, H. J., et al. (2015). Involvement of cholesterol in Campylobacter jejuni cytolethal distending toxin-induced pathogenesis. *Future Microbiol.* 10, 489–501. doi: 10.2217/fmb.14.119

Li, G. M., Li, Y. G., Yamate, M., Li, S. M., and Ikuta, K. (2007). Lipid rafts play an important role in the early stage of severe acute respiratory syndrome-coronavirus life cycle. *Microbes Infect.* 9, 96–102. doi: 10.1016/j.micinf.2006.10.015

Lin, C. D., Lai, C. K., Lin, Y. H., Hsieh, J. T., Sing, Y. T., Chang, Y. C., et al. (2011). Cholesterol depletion reduces entry of Campylobacter jejuni cytolethal distending toxin and attenuates intoxication of host cells. *Infect. Immun.* 79, 3563–3575. doi: 10.1128/IAI.05175-11

Low, C., Jegerschold, C., Kovermann, M., Moberg, P., and Nordlund, P. (2012). Optimisation of over-expression in E. coli and biophysical characterisation of human membrane protein synaptogyrin 1. *PLoS One* 7, e38244. doi: 10.1371/journal.pone.0038244

Lu, Y., Liu, D. X., and Tam, J. P. (2008). Lipid rafts are involved in SARS-CoV entry into Vero E6 cells. *Biochem. Biophys. Res. Commun.* 369, 344–349. doi: 10.1016/j.bbrc.2008.02.023

Mick, E., Kamm, J., Pisco, A. O., Ratnasiri, K., Babik, J. M., Castaneda, G., et al. (2020). Upper airway gene expression reveals suppressed immune responses to SARS-CoV-2 compared with other respiratory viruses. *Nat. Commun.* 11, 5854. doi: 10.1038/s41467-020-19587-y

Nelson, C. D., Carney, D. W., Derdowski, A., Lipovsky, A., Gee, G. V., O'Hara, B., et al. (2013). A retrograde trafficking inhibitor of ricin and Shiga-like toxins inhibits infection of cells by human and monkey polyomaviruses. *mBio* 4, e00729–e00713. doi: 10.1128/mBio.00729-13

Nonnenmacher, M. E., Cintrat, J. C., Gillet, D., and Weber, T. (2015). Syntaxin 5-dependent retrograde transport to the trans-Golgi network is required for adeno-associated virus transduction. *J. Virol.* 89, 1673–1687. doi: 10.1128/JVI.02520-14

Oksayan, S., Ito, N., Moseley, G., and Blondel, D. (2012). Subcellular trafficking in rhabdovirus infection and immune evasion: a novel target for therapeutics. *Infect. Disord. Drug Targets* 12, 38–58. doi: 10.2174/187152612798994966

Ou, X., Liu, Y., Lei, X., Li, P., Mi, D., Ren, L., et al. (2020). Characterization of spike glycoprotein of SARS-CoV-2 on virus entry and its immune cross-reactivity with SARS-CoV. *Nat. Commun.* 11, 1620. doi: 10.1038/s41467-020-15562-9

Regan, A. D., and Whittaker, G. R. (2013). Entry of rhabdoviruses into animal cells. *Adv. Exp. Med. Biol.* 790, 167–177. doi: 10.1007/978-1-4614-7651

Scudellari, M. (2021). How the coronavirus infects cells - and why Delta is so dangerous. *Nature* 595, 640–644. doi: 10.1038/d41586-021-02039-y

Scuron, M. D., Boesze-Battaglia, K., Dlakic, M., and Shenker, B. J. (2016). The cytolethal distending toxin contributes to microbial virulence and disease pathogenesis by acting as a tri-perditious toxin. *Front. Cell Infect. Microbiol.* 6, 168. doi: 10.3389/fcimb.2016.00168

Shang, J., Wan, Y., Luo, C., Ye, G., Geng, Q., Auerbach, A., et al. (2020). Cell entry mechanisms of SARS-CoV-2. *Proc. Natl. Acad. Sci. U.S.A.* 117, 11727–11734. doi: 10.1073/pnas.2003138117

Shenker, B. J., Besack, D., McKay, T., Pankoski, L., Zekavat, A., and Demuth, D. R. (2005). Induction of cell cycle arrest in lymphocytes by Actinobacillus actinomycetemcomitans cytolethal distending toxin requires three subunits for maximum activity. *J. Immunol.* 174, 2228–2234. doi: 10.4049/jimmunol.174.4.2228

Shenker, B. J., Boesze-Battaglia, K., Zekavat, A., Walker, L., Besack, D., and Ali, H. (2010). Inhibition of mast cell degranulation by a chimeric toxin containing a novel phosphatidylinositol-3,4,5-triphosphate phosphatase. *Mol. Immunol.* 48, 203–210. doi: 10.1016/j.molimm.2010.08.009

Shenker, B. J., Dlakic, M., Walker, L. P., Besack, D., Jaffe, E., LaBelle, E., et al. (2007). A novel mode of action for a microbial-derived immunotoxin: the cytolethal distending toxin subunit B exhibits phosphatidylinositol 3,4,5-triphosphate phosphatase activity. *J. Immunol.* 178, 5099–5108. doi: 10.4049/jimmunol.178.8.5099

Shenker, B. J., Hoffmaster, R. H., McKay, T. L., and Demuth, D. R. (2000). Expression of the cytolethal distending toxin (Cdt) operon in Actinobacillus actinomycetemcomitans: evidence that the CdtB protein is responsible for G2 arrest of the cell cycle in human T cells. *J. Immunol.* 165, 2612–2618. doi: 10.4049/jimmunol.165.5.2612

Shenker, B. J., Korostoff, J., Walker, L. P., Zekavat, Z., Dhingra, A., and Kim, T. J. (2024). Aggregatibacter actinomycetemcomitans Cytolethal Distending Toxin Induces Cellugyrin-(Synaptogyrin 2) Dependent Cellular Senescence in Oral Keratinocytes. *Pathogens* 13 (2), 155. doi: 10.3390/pathogens13020155

Shenker, B. J., Walker, L. P., Zekavat, A., Dlakic, M., and Boesze-Battaglia, K. (2014). Blockade of the PI-3K signalling pathway by the Aggregatibacter actinomycetemcomitans cytolethal distending toxin induces macrophages to synthesize and secrete pro-inflammatory cytokines. *Cell Microbiol.* 16, 1391–1404. doi: 10.1111/cmi.2014.16.issue-9

Stenius, K., Janz, R., Sudhof, T. C., and Jahn, R. (1995). Structure of synaptogyrin (p29) defines novel synaptic vesicle protein. *J. Cell Biol.* 131, 1801–1809. doi: 10.1083/jcb.131.6.1801

Sun, Q., Qi, X., Zhang, Y., Wu, X., Liang, M., Li, C., et al. (2016). Synaptogyrin-2 promotes replication of a novel tick-borne bunyavirus through interacting with viral nonstructural protein NSs. *J. Biol. Chem.* 291, 16138–16149. doi: 10.1074/jbc.M116.715599

Walker, L. R., Engle, T. B., Vu, H., Tosky, E. R., Nonneman, D. J., Smith, T. P. L., et al. (2018). Synaptogyrin-2 influences replication of Porcine circovirus 2. *PloS Genet.* 14, e1007750. doi: 10.1371/journal.pgen.1007750

Wan, Y., Shang, J., Graham, R., Baric, R. S., and Li, F. (2020). Receptor recognition by the novel coronavirus from wuhan: an analysis based on decade-long structural studies of SARS coronavirus. *J. Virol.* 94. doi: 10.1128/JVI.00127-20

Xu, Z., Huang, G., and Kandror, K. V. (2006). Phosphatidylinositol 4-kinase type IIalpha is targeted specifically to cellugyrin-positive glucose transporter 4 vesicles. *Mol. Endocrinol.* 20, 2890–2897. doi: 10.1210/me.2006-0193

Zhou, M., Zhang, Q., Zhao, J., and Jin, M. (2012). Haemophilus parasuis encodes two functional cytolethal distending toxins: CdtC contains an atypical cholesterol recognition/interaction region. *PloS One* 7, e32580. doi: 10.1371/journal.pone.0032580